Cell Communication and Signaling

RESEARCH

Open Access

From cell lines to the clinic: identifying a urinary BlCa-EV signature through comparative proteomics of bladder cancer lysates and extracellular vesicles

Catarina Lourenço[1,2,3,4], Vera Constâncio[1,2], Nuno Tiago Tavares[1,2,3], Sara Monteiro-Reis[1,2], Rui Silva-Santos[1,5], João Lobo[1,2,5], Ângela Carvalho[4,6] and Carmen Jerónimo[1,2,7*]

Abstract

Background There is an urgent need for the development of innovative diagnostic and therapeutic strategies in bladder cancer (BlCa) management, due to its significant incidence, mortality, and morbidity. Extracellular vesicles (EVs) constitute promising candidates as biomarkers, as their cargo is highly protected from degradation, and they can be isolated non-invasively from urine. Furthermore, they play a pivotal role in intercellular communication that drives disease progression, making them suitable candidates for tailored therapy approaches.

Methods We employed high-throughput mass-spectrometry to perform a comprehensive proteomic analysis of cell lysates and matched EVs. EVs were isolated from six distinct human BlCa cell lines, representatives of the complete disease spectrum, to identify a BlCa-EV associated signature. The translational ability of this signature was analyzed in urinary EV (uEV) samples from BlCa patients and healthy controls.

Results This study established a new lysate-to-EV signature that is common to all malignant cell lines. Afterwards, this profile was analyzed in BlCa uEVs, identifying a robust and novel 13-protein BlCa-enriched signature, which includes ITGA2, ITGA6, SCRIB, and TFRC.

Conclusion We unveiled a novel, EV-derived protein signature that has potential to be further applied for future functional studies, non-invasive diagnostic assays and targeted therapeutic interventions against BlCa.

Keywords Bladder cancer, Extracellular vesicles, Cell lines, Proteomics, Urine

*Correspondence:
Carmen Jerónimo
carmenjeronimo@ipoporto.min-saude.pt

Full list of author information is available at the end of the article

© The Author(s) 2026. **Open Access** This article is licensed under a Creative Commons Attribution-NonCommercial-NoDerivatives 4.0 International License, which permits any non-commercial use, sharing, distribution and reproduction in any medium or format, as long as you give appropriate credit to the original author(s) and the source, provide a link to the Creative Commons licence, and indicate if you modified the licensed material. You do not have permission under this licence to share adapted material derived from this article or parts of it. The images or other third party material in this article are included in the article's Creative Commons licence, unless indicated otherwise in a credit line to the material. If material is not included in the article's Creative Commons licence and your intended use is not permitted by statutory regulation or exceeds the permitted use, you will need to obtain permission directly from the copyright holder. To view a copy of this licence, visit http://creativecommons.org/licenses/by-nc-nd/4.0/.

Graphical Abstract

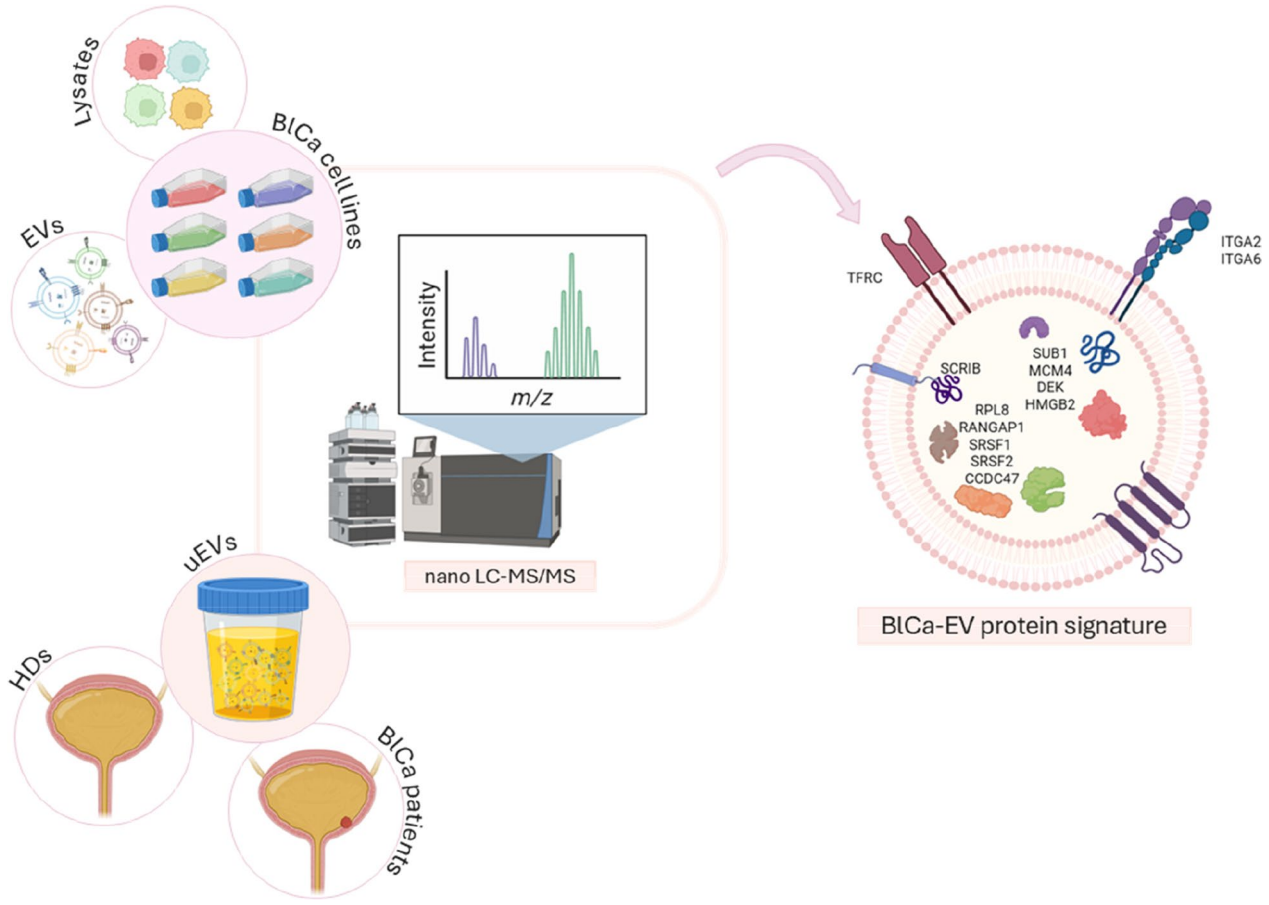

Introduction

Bladder cancer (BlCa) is among the 10 most common cancers in the world [1], presenting a significant health burden due to increasing incidence and mortality rates, coupled with the limitations of current diagnostic and monitoring approaches [2]. While non-muscle-invasive bladder cancer (NMIBC) often carries a favorable prognosis, it presents high recurrence and progression rates to muscle invasive disease [3]. Consequently, these patients are subjected to lifelong, invasive surveillance procedures [4]. Conversely, muscle-invasive bladder cancer (MIBC) tumors are aggressive, with poor outcomes, often showing limited therapeutic response [5]. Although less invasive alternatives exist, their insufficient sensitivity severely hampers their clinical utility [6–9]. Altogether, the combination of all these factors makes BlCa one of the cancers with the highest lifetime treatment costs per patient [10]. Hence, there is an urgent and unmet need for novel non-invasive diagnostic and monitoring alternatives that can reduce both the financial burden and morbidity associated with BlCa management.

Extracellular vesicles (EVs) are nano-lipidic structures, pivotal in intercellular communication [11]. These particles encapsule diverse molecular cargo – including proteins, lipids, and nucleic acids – which are often a reflection of its parental cell status [12]. These vesicles have emerged as a promising source of non-invasive biomarkers since they are readily accessible and highly stable in biofluids [13]. In BlCa specifically, urine presents itself as a golden EV biomarker source, since it allows for a completely non-invasive and painless collection method of a biofluid that has direct contact with the tumor [14]. Furthermore, tumor-derived EVs (tEVs) play crucial roles in remodeling the tumor microenvironment and promoting cancer progression [15], while also having enormous potential for early cancer detection, as they are released even by pre-malignant lesions [16]. However, targeting and capturing tEVs remains challenging due to the high complexity of biological samples, which encompass factors such as the contribution of different EV sources, biological contaminants and patient heterogeneity. Moreover, diverse pre-analytical parameters need to be considered, such as time of collection, diet, sample processing,

amongst other variables [17]. These factors generate substantial confounding markers while potentially masking genuine disease-specific signals. Established cancer cell lines provide a rich and controlled source of material that allow for identification of tumor-specific EV signatures, without the background noise of confounding variables that are inherent to patient-derived biological fluids [18].

In this study, we employed advanced high-throughput spectrometry to comprehensively characterize the proteome of BlCa cell lines, ensuring that the analyzed molecular cargo was intrinsically related to the malignant phenotype. Crucially, the side-by-side proteomic comparison of the parental cell lysate and the matched secreted EVs was used to identify a core BlCa-associated EV signature and unveil the proteins that are actively encapsulated and exported via vesicles [19, 20]. Comparison of this signature with BlCa patient uEVs, supported BlCa cell lines as appropriate models to study BlCa-derived EVs with biological and clinical accuracy. This work has the potential to uncover EV-based tumor communication mechanisms, as well as new non-invasive diagnostic and management biomarkers and potential therapeutic targets.

Materials and methods

Cell culture

Six BlCa cell lines (SW780, RT112, T24, J82, UMUC3 and 253 J) presenting different characteristics of the disease spectrum – from low to high grade lesions, across different stages and molecular subtypes – were used [21–23]. All cell lines were purchased from ATCC and grown using the recommended medium (Biochrom-Merck, Berlin, Germany) supplemented with 10% fetal bovine serum (FBS, Biochrom) and 1% penicillin/streptomycin (GBICO, Invitrogen) at 37 °C and 5% CO^2 (Table 1, Figure S1A). All cell lines were authenticated, and passage number was kept below 60, with maximum 10 passages at each time cells were kept in culture. Mycoplasma test was regularly performed (every two weeks) in all cell lines, using TaKaRa PCR Mycoplasma Detection Set (Clontech Laboratories, Mountain View, CA, EUA).

For EV isolation, cell lines were cultured in five 150 mm Petri dishes, each containing 20 ml of medium, for 72 h, with a previously optimized cell density so 80–90% confluency would be achieved at the end of experiment. The culture medium was supplemented with EV-free fetal bovine serum (FBS), which had been prepared beforehand by depleting vesicles via ultracentrifugation (UC) at 100,000 g for 70 min (min). Cell viability was assessed at the time of collection and consistently exceeded 90% across all conditions (Supplementary Table 1). After culturing, the cells and their respective conditioned medium (CM) were harvested and processed. Cells were washed with PBS after trypsinization and then lysed using RIPA lysis buffer supplemented with 1x protease inhibitors cocktail (PIC). The cell lysates were incubated for 30 min at 4 °C and subsequently centrifuged at 12,000 rpm for 20 min at 4 °C, with the resulting supernatant being collected. For the CM, cellular debris was eliminated via two sequential centrifugation steps at 10 °C: first at 500 g for 10 min, followed by a second spin at 3,000 g for 20 min. Both the cell lysates and the processed CMs were stored at -80 °C until further use.

Table 1 Clinicopathologic characterization of human BlCa cell lines [23]

Cell Line	Grade	Stage	Subtype	Gender	Culture medium
SW780	G1	NR	Luminal	F	DMEM
RT112	G2	pTa	Luminal	F	RPMI-1640
T24	G3	pTa	NR	F	RPMI-1640
J82	G3	pT3	Basal	M	MEM
UMUC3	G4	≥pT2	Basal	M	DMEM
253 J	G4	pT4	Basal	M	DMEM

EVs isolation from BlCa cell lines

100 mL of CM was used to perform EV isolation, using differential UC, as previously described [6, 24, 25]. Firstly, CM was ultracentrifuged at 12,000 g for 20 min, to deplete large EVs, then another UC at 100,000 g for 70 min was performed to pellet small EVs. All UCs were performed at 10 °C in an Optima XE-100 Ultracentrifuge (Beckman Coulter, California, EUA) using the 45Ti rotor (Beckman Coulter, California, EUA). Finally, EV pellets were resuspended with 200 µL of 0.22 µm filtered PBS (f-PBS) and stored at -80 °C after Nanosight tracking analysis (NTA) characterization.

Urine supernatant processing and uEV isolation

Urine samples from a retrospective cohort of both BlCa patients and healthy donors (HDs) were retrieved from the IPO Porto Biobank. Patients' urine was collected at the time of diagnosis and before any therapy. Donors with matched gender and average age of the patients' group were selected, to ensure comparability. Donors with matched gender and average age of the patients' group were included, to ensure comparability. All procedures were conducted under the approval of the Ethics Committee of IPO Porto (CES 174/022) and the specific clinicopathological characteristics of the patients and HDs are detailed in Table 2. This study complies with the institutional/national ethical standards, following the 1964 Helsinki declaration and its later amendments or comparable ethical standards. To maintain sample integrity, all processing was initiated within a maximum of three hours of collection. The samples were first centrifuged at 1,000 g for 10 min at 4 °C (without braking) to separate the urine supernatant from any pelleted cells/debris. The

Table 2 Clinical and pathological characteristics of urine samples from BlCa patients and controls used in the study. HG: high grade, is: carcinoma in situ

Sample	Classification	Age	Gender
BlCa1	pTis (urothelial carcinoma in situ)	77	M
BlCa2	pTa, HG papillary urothelial carcinoma	58	M
BlCa3	pTa, HG papillary urothelial carcinoma	73	F
BlCa4	pT3, invasive urothelial carcinoma, high grade	81	F
BlCa5	pT1, HG papillary urothelial carcinoma	53	F
BlCa6	≥pT2, HG invasive urothelial carcinoma, conventional (5%) combined with neuroendocrine carcinoma (> 50%)	85	M
HD1	--	66	M
HD2	--	59	F
HD3	--	63	F
HD4	--	63	M
HD5	--	64	F
HD6	--	61	M

resulting supernatant was then promptly stored at -80 °C until further analysis.

After thawing, a 9 mL aliquot of the urine supernatant was subjected to another centrifugation step at 3,000 g for 20 min to remove any remaining sediments. For the subsequent UC protocol, samples were transferred to a thick wall polycarbonate tube (Ref: 355631, Beckman Coulter, California, USA) and diluted with f-PBS to a final volume of 10 mL.

The process of differential UC was then used to isolate urinary EVs (uEVs). First, a centrifugation step at 12,000 g for 20 min at 10 °C was performed to pellet larger vesicles. The resulting supernatant was then subjected to a final UC step at 100,000 g for 70 min (at 10 °C) to isolate the smaller EVs. The UCs were carried out in an Optima XE-100 Ultracentrifuge (Beckman Coulter, California, USA) using the 70Ti rotor. Following the final UC, the supernatant was discarded, and the isolated uEV pellets were resuspended in 100 µL f-PBS into a 1.5 mL low-binding tube. After NTA characterization, samples were then stored at -80 °C until further use.

EV characterization

Protein quantification

Protein concentration of cell lysates and EV samples was quantified using the BCA™ Protein Assay Kit (ThermoFisher Scientific, Waltham, Massachusetts, USA), following manufacturer's instructions. The plates were read in a microplate reader (BMG LABTEC, Ortenberg, German) at 562 nm in a FLUOstar Omega.

Nanosight tracking analysis

For assessment of particle size and concentration, we employed NTA using a Nanosight NS300 system equipped with a red laser (Malvern Panalytical, United Kingdom). Three to six cell line derived-EV replicates and 12 uEV samples were analyzed by this technique. Briefly, EV samples were diluted in f-PBS and introduced into a 1 mL syringe. Five 30 s videos were recorded during the analysis, maintaining a continuous syringe pump flow rate of 3 units. Throughout the experiments, the temperature was maintained at a targeted 25 °C. For all captures, a screen gain of 9 and a camera level of 10 were consistently applied. The results obtained were validated with a minimum of 1,000 total tracks and a particle count ranging between 10 and 50 per frame. The recorded videos were subsequently analyzed using NTA software version 3.4. Particle concentration was normalized to volume of urine.

Transmission electron microscopy

EV morphology was assessed by transmission electron microscopy (TEM), using negative staining. Firstly, 10 µL of diluted EVs were mounted on Formvar/carbon film-coated mesh nickel grids (Electron Microscopy Sciences, Hatfield, PA, USA) and left standing for 2 min. Afterwards, 10 µL of 1% uranyl acetate were added onto the grids with excess liquid removed. Visualization was carried out on a JEOL JEM 1400 microscope (Tokyo, Japan) at 120 kV and images were recorded using the digital camera Orious 1100 W (Tokyo, Japan).

Mass spectrometry

Three replicates from cell line-derived samples, and 12 human urine EV samples were analyzed by mass spectrometry (MS). Approximately 40 µg of total lysate protein or total EV protein were processed for proteomic analysis. Samples were first incubated at 95 °C for 10 min at 1,000 rpm in a solution containing 100 mM Tris (pH 8.5), 1% (w/v) sodium deoxycholate (SDC), 10 mM tris (2-carboxyethyl) phosphine hydrochloride (TCEP) and 40 mM 2-chloroacetamide (CAA). Following the solid-phase-enhanced sample-preparation (SP3) protocol, samples were enzymatically digested with trypsin/LysC as previously described [26].

Protein identification and quantification was performed using nanoscale liquid chromatography-tandem mass spectrometry (nanoLC-MS/MS). The instrumentation consisted of a Vanquish neoliquid chromatography system coupled to an Eclipse Tribrid Quadrupole Ion trap Orbitrap mass spectrometer along with a High-field asymmetric waveform ion mobility spectrometry – FAIMS equipment (Thermo Scientific). 250 nanograms of peptides were quantified for each sample and data acquisition was performed following the previously established methods [26].

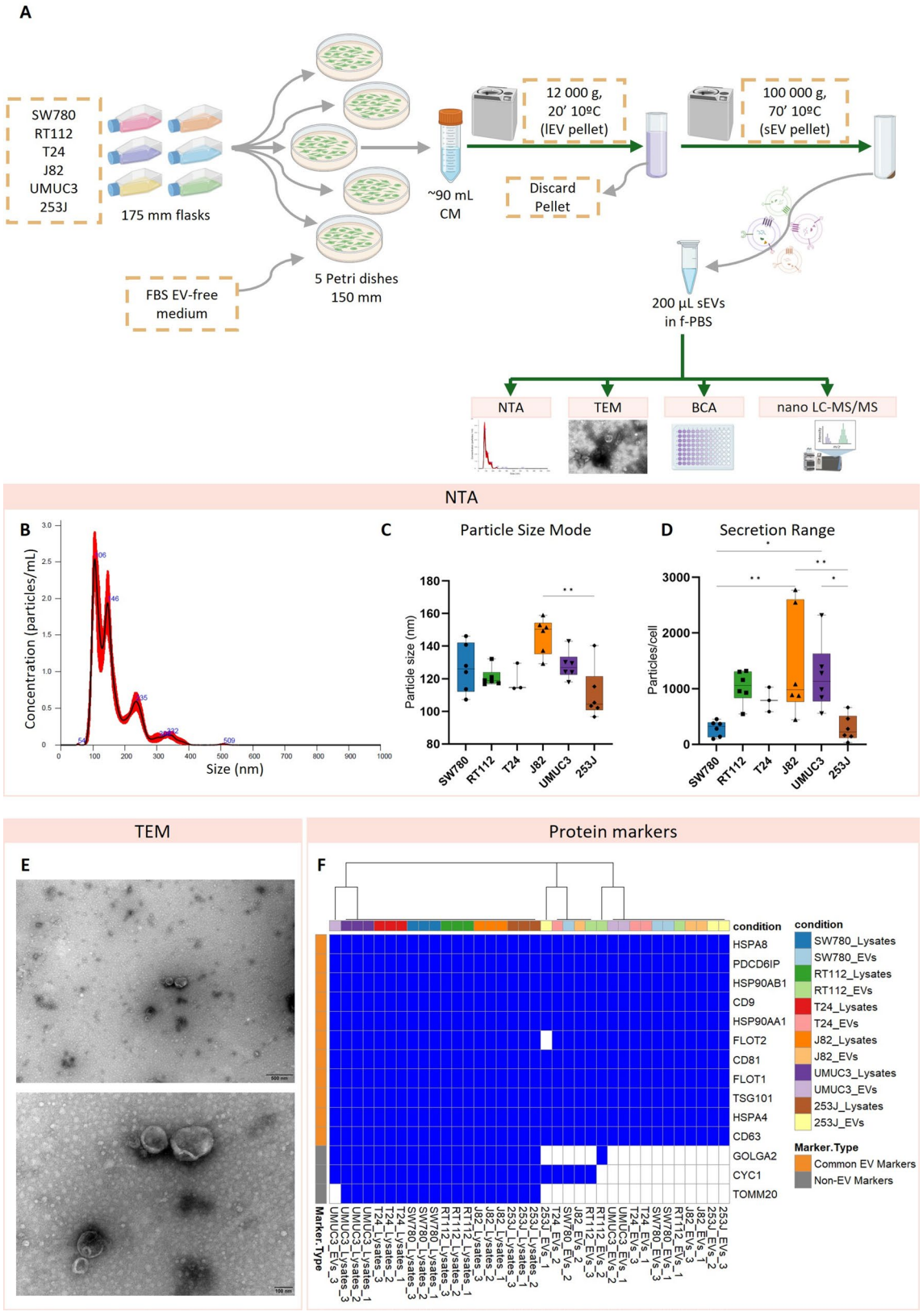

Fig. 1 (See legend on next page.)

(See figure on previous page.)

Fig. 1 Isolation and characterization of BlCa cell line derived-EVs. **A** Schematic representation of the study workflow with UC protocol and EV characterization. Created with BioRender.com. **B** Representative NTA profile showing size distribution of BlCa-derived EVs. **C** EV mode size distribution and (**D**) secretion range (number of particles released per cell) across the different cell lines. Statistical analysis was performed using the Kruskal-Wallis test, * $p < 0.05$; ** $p < 0.01$. Measurements of 3 to 6 replicates. **E** Representative TEM image EVs, derived from SW780 cell line, were acquired at 25,000x magnification (scale bar: 500 nm) and 100,000x magnification (scale bar:100 nm). **F** Positivity (blue boxes) for conventional EV and non-EV markers across all samples based on LC-MS/MS data

Bioinformatic analysis

Data was processed using Proteome Discoverer 3.1.0.638 software (Thermo Scientific) and searched against the UniProt database for the *Homo sapiens* reviewed proteome (2024_01 with 20,418 entries). A common protein contaminant list search from MaxQuant was also included in the analysis.

The *Results* data file obtained from Proteome Discoverer, R software (v4.4.2) was used for processing, quality control and analysis of the study proteomic data. Only proteins with high False Discovery Rate (FDR) confidence (1%), absent from the contaminant list and with at least two unique peptides were retained. Moreover, to ensure data quality and reliability, only proteins with at least two peptide spectrum matches (PSMs; "High") were considered as identified by MS/MS. Therefore, abundancies from proteins with PSMs < 2 – "Peak Found" or "n/a" entries in "Found in sample" – were set to 0 in the corresponding "Abundance (Normalized)" column. Missing values in "Abundance (Normalized)" of identified proteins were also replaced by 0. To increase robustness, only proteins present in all replicates within at least one condition were kept. For protein frequency analysis, proteins' presence or absence was assessed without considering abundance. For cell lines, a protein was considered detected within a condition if it was present in 100% of replicates of said condition (Figure S2). Regarding uEVs, only proteins present in 50% of HDs or BlCa samples were kept.

Package "ggplot2" was used to generate bar and box plots, to identify protein counts across different samples. To account for protein overlap among experimental groups an Upset plot was generated by "UpSetR" package and "eulerr" package was used to generate the Euler diagrams for overlap between lysate and EV from each cell line. For protein abundance, abundance values equal to 0 were imputed with the minimum non-zero abundance value per sample divided by 3 to facilitate log2 transformation. Principal Component Analysis (PCA) evaluated sample clustering using the "factoextra" package. Using the "pheatmap" package, hierarchical clustering heatmap was generated, and Pearson correlation heatmap was generated to evaluate the correlation between samples. Condition annotations were incorporated for visualization. Statistical significance of log2-transformed protein abundance for each of protein identified as BlCa-exclusive was determined using the Wilcoxon rank-sum test. Enrichment analyses for Biological Processes (BP) of Gene Ontology (GO) were performed using the "clusterProfiler" package. The "enrichGO" function was applied with multiple testing correction with the Benjamini-Hochberg method. Subcellular localization was retrieved from the Human Protein Atlas (HPA), using the "HPAanalyze" package.

Statistics

Statistical analyses for particle concentration and sizes were performed using GraphPad Software (GraphPad Software, Boston, MA, USA). Kolmogorov-Smirnov test was performed to check normality. Comparisons between groups were performed using the non-parametric test Mann–Whitney U test. *P*-values lower than 0.05 were considered statistically significant, with $^{*}p < 0.05$ and $^{**}p < 0.01$, $^{***}p < 0.001$, $^{****}p < 0.0001$.

Results

EV characterization

EVs representing different characteristics of BlCa disease (Table 1) were isolated by UC and characterized in accordance with the Minimal information for studies of extracellular vesicles (MISEV) guidelines [27] (Fig. 1A). NTA showed that particle size mode ranged from 100 to 160 nm, with no significant differences among EVs derived from the various cell lines, except for 253 J-derived EVs, which were significantly smaller than those from J82 (Fig. 1B-C, $p = 0.0025$). Curiously, J82 and UMUC3, typically aggressive phenotype cell lines, secreted more particles than SW780 and 253 J (Fig. 1D), suggesting that secretion pattern was independent of tumor grade, since SW780 represents the lowest stage among the analyzed cell lines, while 253 J comes from an aggressive and metastatic origin. TEM showed cup-shaped vesicular structures within the expected EV size range (Fig. 1E, S1A). Regarding protein markers, all replicates expressed conventional EV-associated proteins, except for one 253 J-EV replicate that lacked Flotillin 2 (FLOT2). As expected, contaminant markers were detected in the cell lysates but were largely absent from the corresponding cell-derived EVs (Fig. 1F), showing the successful isolation of our EV population.

Proteome characterization

From our proteomic study, 6,886 identified proteins were absent from the contaminants list, with high FDR

and presented at least two unique peptides. To increase reliability and biological confidence, while minimizing the impact of stochastic noise or sample-specific contaminants, 6,613 proteins that were consistently present across all biological replicates of at least one cell lysate or derived EV condition were considered for further analysis.

To assess global similarities and differences across the six cell line lysates and their derived EVs, PCA was performed (Fig. 2A). Sample type – lysate or EV – was the dominant factor influencing clustering (PC1 54.8%). PC2 then separates lysates into two clusters (PC2 10.7%): one comprising SW780, RT112 and J82, and the other UMUC3, 253 J and T24. Furthermore, all lysate replicates derived from the same cell line clustered together. Moreover, while EV samples clustered apart from cell lysates, J82-derived EVs further segregated from other EV samples. The sample type separation was also evident in the heatmap, which clearly distinguished lysates from EVs (Fig. 2B).

In agreement with PCA, unsupervised hierarchical clustering of Pearson correlations showed perfect segregation of lysate replicates. In contrast, EV replicates exhibited high mutual correlation, even across different cell lines (Fig. 2C). Notably, lysate-to-EV showed weak correlations ($r = 0.212$ to 0.350), across matched lysate to EV cell line (Supplementary Table 2).

Together, these analyses reveal two proteomic subtypes among the cell lysates, while EVs display greater heterogeneity, with J82-EVs emerging as a distinct "outlier" within the EV compartment.

BlCa cell line selective packaging and proteomic signatures

Considering that different cell lines were analyzed and that cargo packaging can vary among them, we evaluated the degree of overlap between lysate and EV proteomes for each cell line (Fig. 3A-B and S3). Interestingly, the proportion of shared proteins was similar across all cell lines, with around 25% (~ 1,200 proteins) of the proteins being common to both lysates and EVs (Supplementary Table 3). In fact, almost 80% of lysate proteome is absent from EVs, whereas, in contrast, EVs share 80% of proteins with lysates proteome (Supplementary Table 4). As expected, these results show that EVs do mirror the proteomic composition of their cells of origin.

Regarding protein number, lysates displayed a substantially higher number of detected proteins compared with EVs. Cell lysates presented around 5,000 different proteins, with 253 J presenting the greatest diversity (5,120 proteins). In contrast, EVs contained almost half as many proteins – about 2,000 proteins – with J82-derived EVs presenting the lowest amount (1,561 proteins) (Fig. 3C, S4A-B; Supplementary Table 5).

The reliability of the proteins found in our analysis was validated by comparison against publicly available databases. For cell lysates, the majority of proteins overlapped with those reported in a previous proteomic analysis of BlCa cell line lysates [28]. Five out of the six cell lines were common between the two studies, and nearly 3,500 proteins were present in both datasets, representing 89.5% of the proteins identified by Puttamalesh and colleagues (Figure S5A). For EVs, comparison with Exocarta [29] and Vesiclepedia [30] databases showed that our EV samples contained 73 of the "Top 100" EV markers listed in both databases, along with an additional 37 proteins appearing in at least one of the two lists (Figure S5B). Additionally, when specifically examining the 374 BlCa cell-derived EV proteins present in these databases, most proteins – 275 – were also detected in our EV dataset (Figure S5C).

To characterize the protein content expressed across the different cell lines and to assess whether a common protein signature could be identified, we quantified the intersecting proteins among all conditions, both in lysates and EVs. Notably, the largest shared set consisted of 1,424 proteins present exclusively in lysates across all six cell lines. In contrast, 52 proteins were shared among EVs from all six cell lines but were absent from the corresponding lysates. Importantly, 497 proteins were common to every condition, being expressed in all replicates, from all cell line lysates as well as their derived EVs (Fig. 3C). Additionally, the correlation between matching lysate and EVs increased from 0.292, in the full proteome, to 0.532 when focusing on commonly detected proteins (Figure S6A and Supplementary Table 6). 156 out of 497 proteins have already been documented in BlCa EV-related databases, showcasing strong alignment between our dataset and previously published findings (Figure S6B). Moreover, from the remaining 341 proteins, consistently detected across all BlCa cell line EVs, some may represent candidate BlCa EV-associated proteins not yet documented in current databases.

As expected, most of the 1,424 lysate exclusive proteins located in the nucleus (40.2%), followed by mitochondria (20.9%) and cytosol (11.7%). On the other hand, EV-exclusive proteins were predominantly associated with vesicles (22.9%), as well as endoplasmic reticulum (ER), Golgi apparatus, and nucleus (each 17.1%). Additionally, none of the EV-exclusive proteins originated from mitochondria. Among the proteins common to all lysates and EVs, the majority were assigned to the cytosol (35.1%), nucleus (22.5%), and plasma membrane (13.7%) (Fig. 4A). To further investigate the functional relevance of these three protein groups, we performed GO enrichment analysis focused on biological processes (Fig. 4B). Using the full 6,613 protein set as a reference list, an over-representation analysis (ORA) was performed. All significant

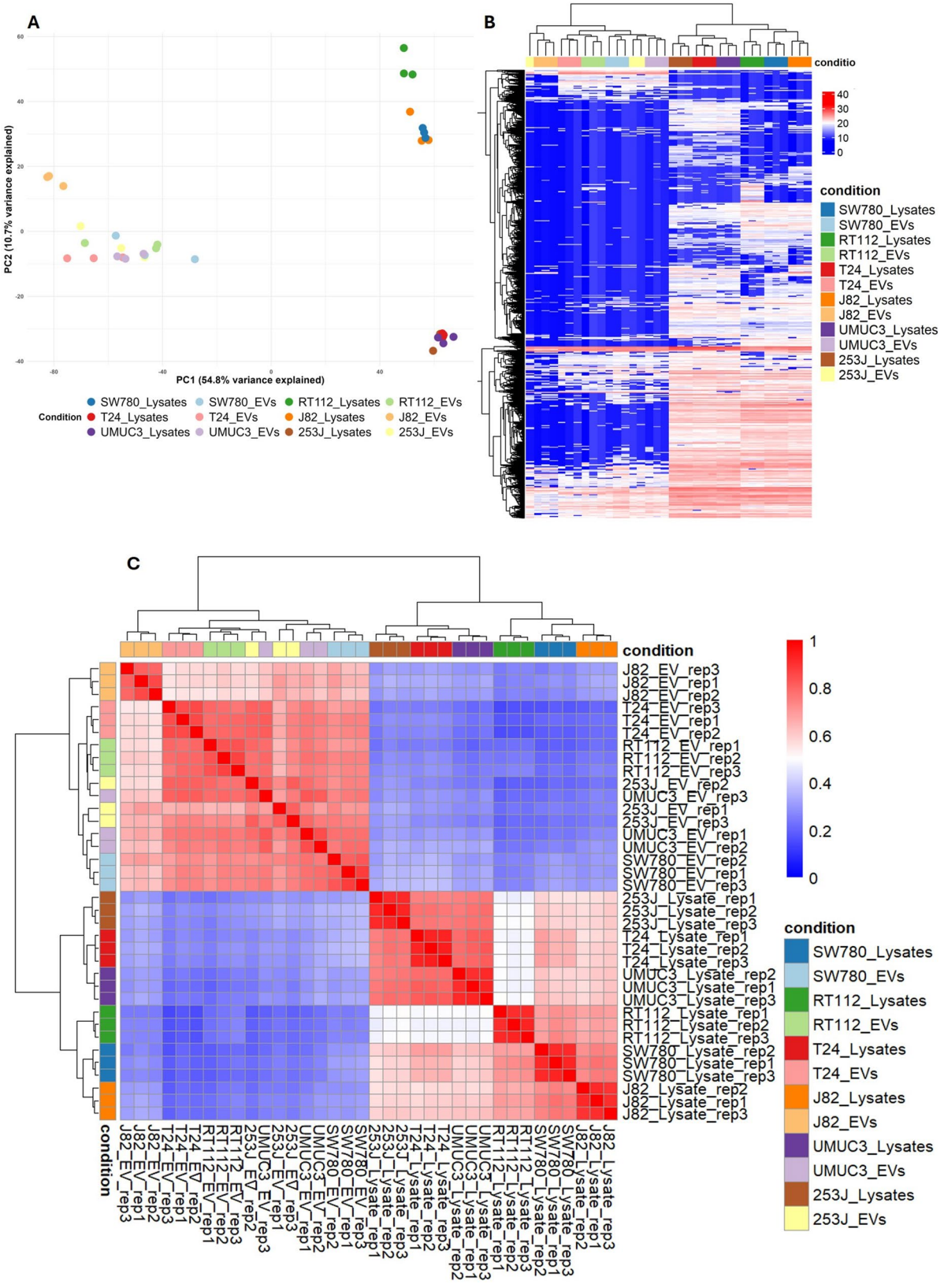

Fig. 2 Proteomic characterization of lysate and EVs derived from different BlCa cell lines. **A** PCA plot of all detected proteins. **B** Unsupervised hierarchical clustering heatmap of samples based on protein expression patterns across all 12 conditions (six cell lysates and matched EVs). The color scale indicates $\log_2$ protein abundance, from high (red) to low (blue) expression. **C** Hierarchical clustering of Pearson correlations, using $\log_2$ protein abundance, among all replicates

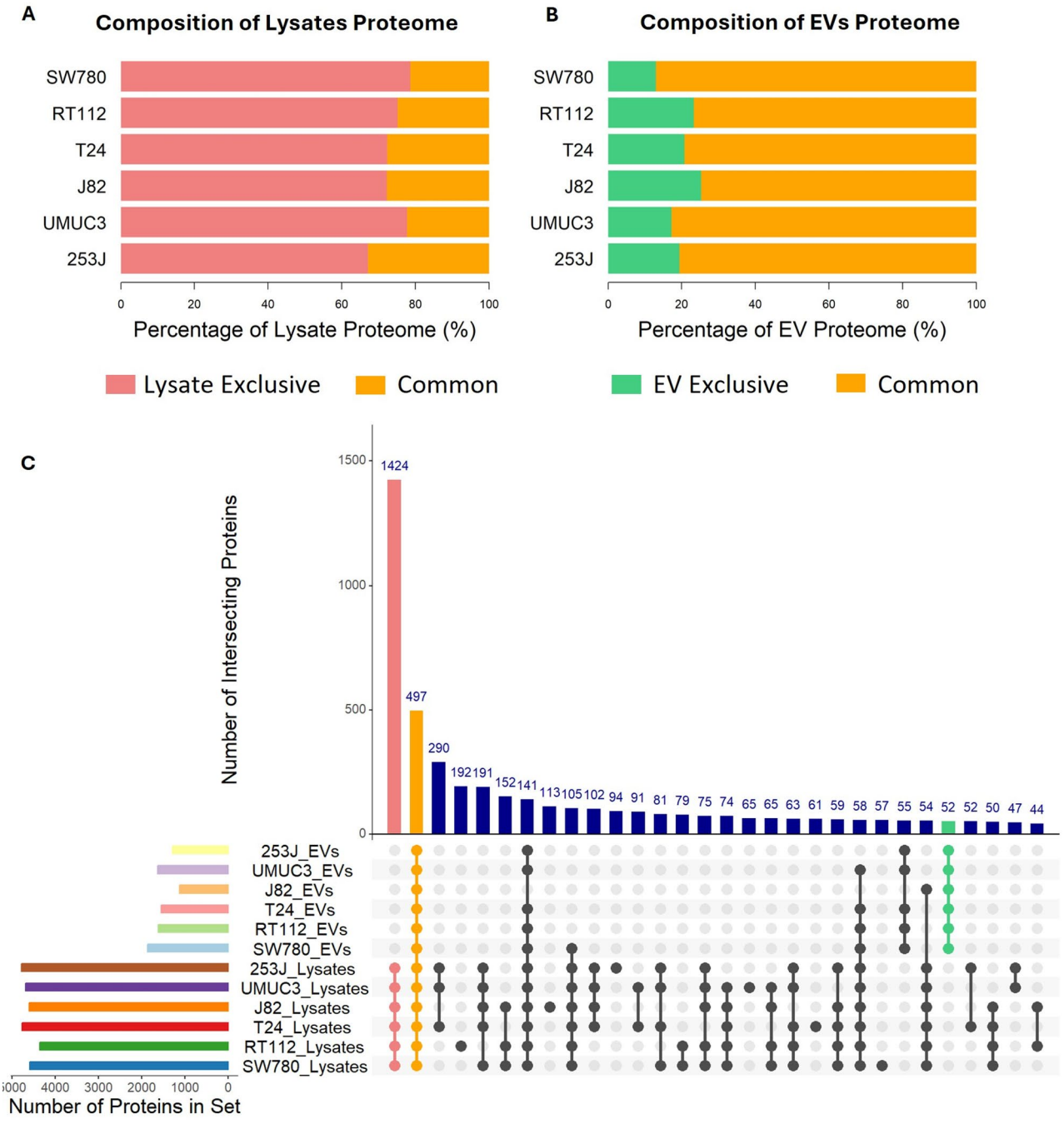

Fig. 3 Overlap of lysate and EV proteome across all BlCa cell lines. **A** Composition of lysate proteome showing percentage of lysate-exclusive and EV overlap proteins. **B** Composition of EV proteome showing percentage of EV-exclusive and lysate overlap proteins. **C** Upset plot showcasing number of proteins per condition, intersections and number of overlapping proteins across different conditions. Highlighted intersections present the 3 different group signatures: Lysate-exclusive, Common (Lysate and EV) and EV-exclusive

GO terms were used to assess the most representative biological clusters (Figure S7).

Proteins shared across all samples were primarily involved in rapid, high-volume cellular activities and motility. These functions are characteristic of highly dynamic cells, such as cancer or migratory immune cells. For instance, terms like "canonical glycolysis" and "NADH metabolic processes" suggest a high energy demand often seen in fast-growing cells. Processes such as "actin cytoskeleton organization", "lamellipodium organization", "import into cell" and "endocytosis" infer about cell shape and movement, while telomere maintenance strongly points to a population of actively dividing or immortalized cells.

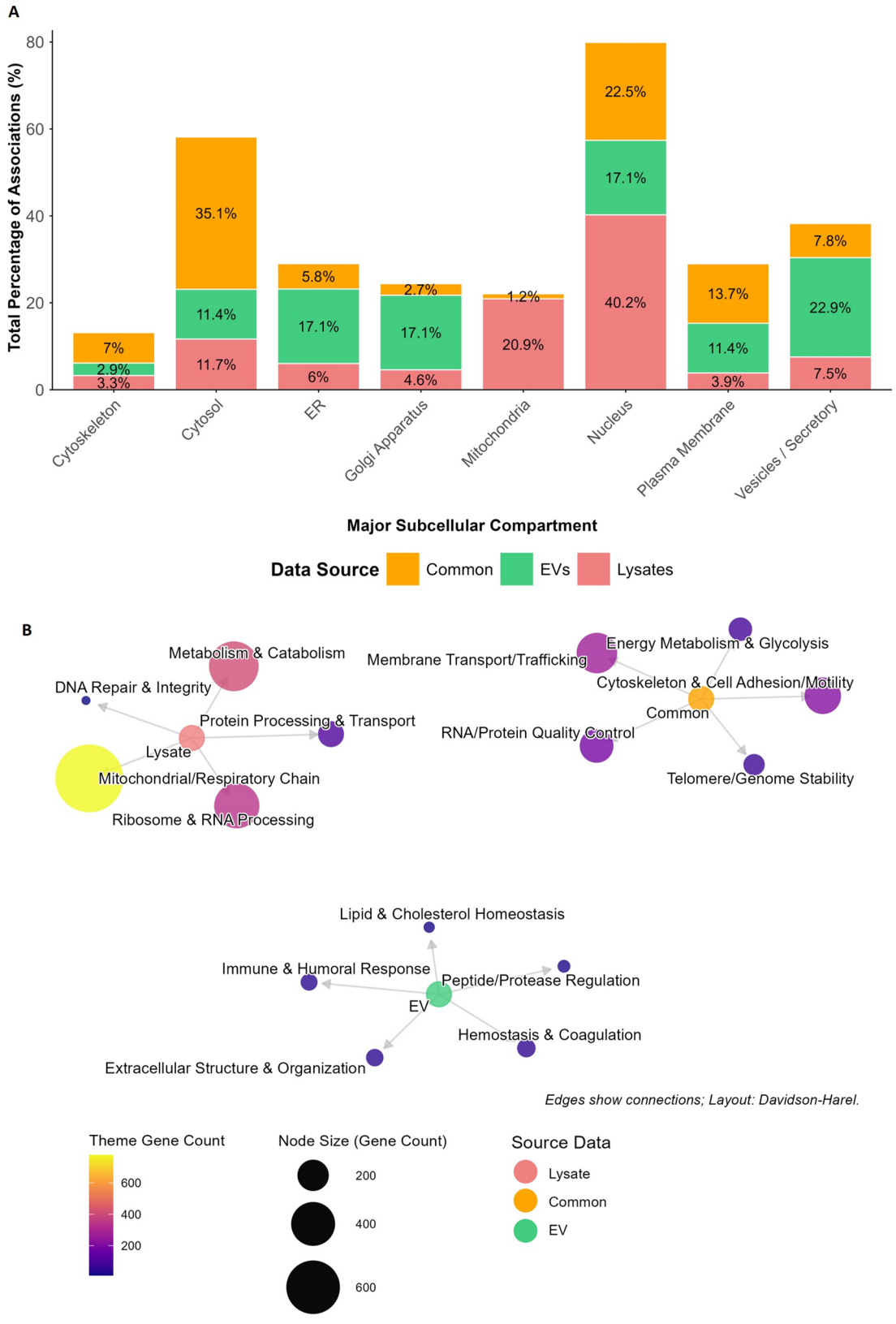

Fig. 4 Subcellular localization and main biological processes across Common, Lysate- and EV-exclusive sets. **A** Distribution of subcellular localization from each group of proteins (in percentages), reflect the experimentally validated cellular localization of each identified protein as determined by the Human Protein Atlas (HPA). **B** Node chart representing the main biological clusters from each dataset. Biological process themes obtained from the significant gene ontology (GO) terms from each group

Lysate-exclusive proteins were enriched in processes associated with metabolic activity, including "oxidative phosphorylation", "cellular respiration", and "ATP synthesis", underscoring the presence of energy-generating machinery. Moreover, terms related to the maintenance and repair of this machinery were prominent, such as "mitochondrial gene expression", "ribosome biogenesis", and "regulation of nucleotide-excision repair". In contrast, EV proteins were predominantly associated with cellular defense and response to damage and threats. Enriched terms included "hemostasis", "fibrinolysis" and "wound healing", indicating active surveillance or inflammatory states, further supported by terms such as "humoral immune response" and "complement activation". Additionally, EV proteins maintained a strong emphasis on cell adhesion and migration, highlighted by terms such as "cell-cell adhesion", "cell-substrate adhesion", and "regulation of cell migration". Notably, all protein groups shared processes related to protein processing, such as "protein folding", "ribosome biogenesis", and "protein processing"; as well as functions related to signaling and molecular trafficking such as "endocytosis", "transport", and "integrin-mediated signaling pathway" (Fig. 4B).

BlCa cell line common proteins are present in the tissues of BlCa patients

To understand whether the signature found in BlCa cell lines reflects patient-derived samples and can therefore have a translational purpose, we cross-checked our proteomics data with a comprehensive proteomic study conducted on formalin-fixed paraffin-embedded (FFPE) bladder tumor tissues from BlCa patients. This study analyzed a cohort of 434 tumor and normal adjacent samples, comprising 242 tumors, ranging from NMIBC Ta low grade to MIBC with lymph node metastasis, and 192 paired normal adjacent mucosae, covering the full spectrum of BlCa disease [31]. Globally, almost 63% of the total proteins identified in both studies overlapped (Fig. 5A), suggesting that BlCa cell line proteins largely mimic what is represented in tissues from BlCa patients. Focusing on proteins shared across the different cell lines, we assessed the overlap between Dressler and colleagues' study and our three defined protein groups (Common, Lysate-exclusive and EV-exclusive). Remarkably, nearly all proteins common to our conditions (486 of 497) were also present in the tissue samples, representing approximately 7.5% of the tissue proteome (Fig. 5B). Moreover, 1,270 of 1,424 lysate-exclusive proteins were also expressed in tissues, accounting for 19.5% of the tissue dataset. Among EV-exclusive proteins, 31 of 52 were found in tissues, representing 0.5% of the tissue proteome. Additionally, another 50.4% of tissue proteins were also present in our study, resulting in approximately 70% of the BlCa tissue proteome being represented within our BlCa cell line proteomics. Together, these findings demonstrate a substantial molecular convergence between BlCa cell line and patient tumor proteomes, indicating that the analyzed in-vitro models capture a large portion of the proteomic landscape observed clinically, thereby supporting their use as relevant translational models.

Translation potential of common proteins in BlCa-uEVs

After identifying 486 proteins common in BlCa cell lines and cancer patients, we ascertained their potential for biomarker and therapeutic strategies. Thus, we evaluated

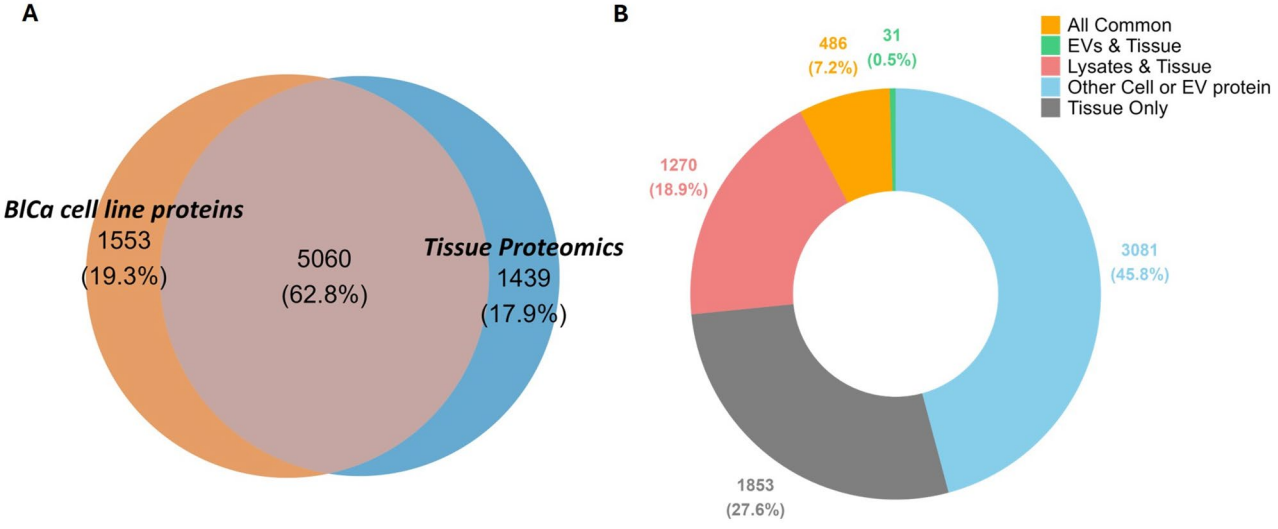

Fig. 5 Presence of BlCa cell line protein signatures in BlCa patient tissues. **A** Venn diagram of our BlCa proteins (6,613) and overlap with proteins identified in BlCa patients tissue proteomic study. **B** Donut chart showing distribution of protein presence/absence from the three different datasets in BlCa patient's tissue proteomics

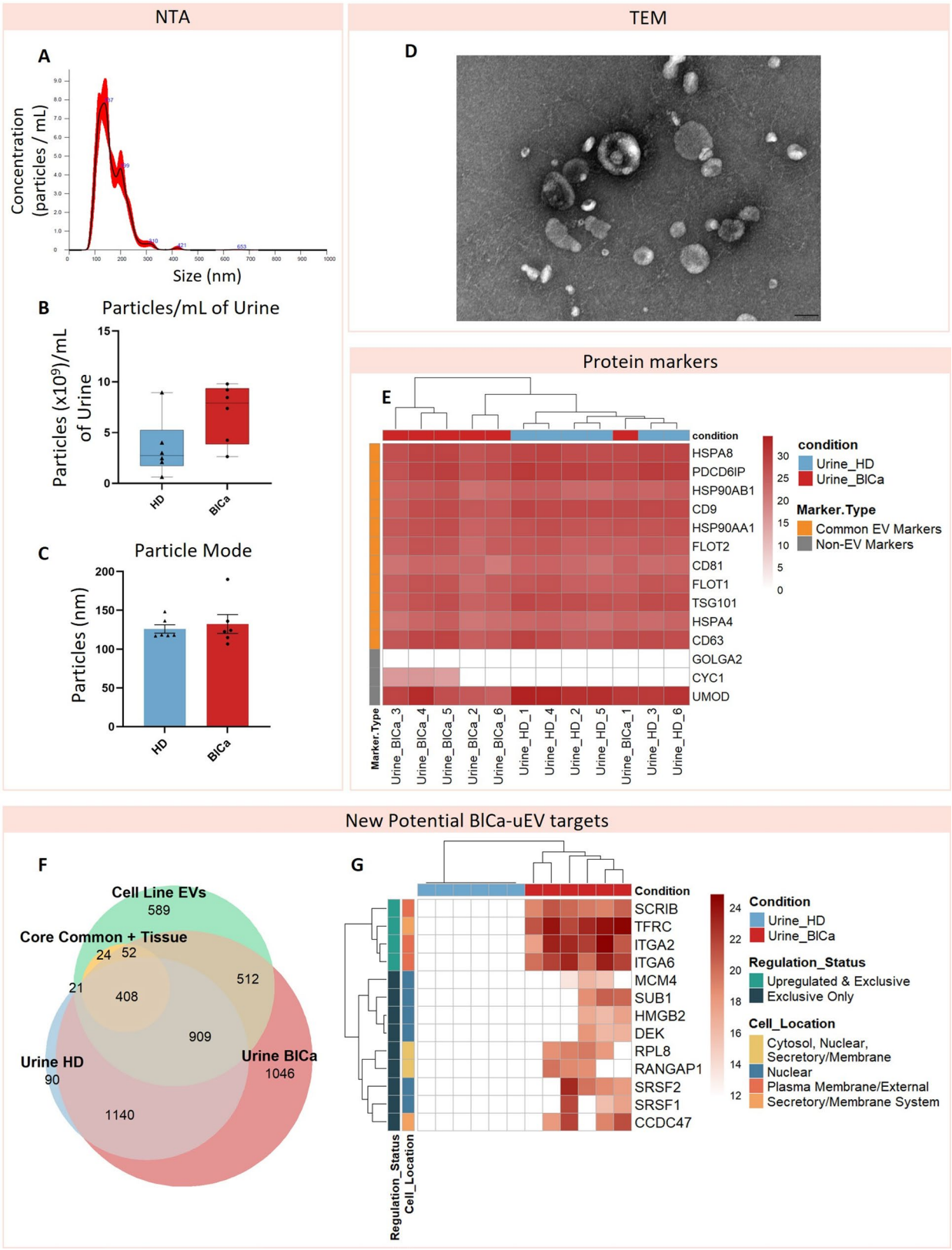

Fig. 6 (See legend on next page.)

(See figure on previous page.)

Fig. 6 Characterization and validation of BlCa-EV cell line derived signature in uEVs of BlCa patients. **A** Representative NTA profile showing size distribution of uEVs. **B** uEV concentration as number of particles per mL of urine and (**C**) uEV mode size distribution. Results are presented as mean ± SEM. **D** Representative TEM images of uEVs at 100,000x magnification (scale bar: 100 nm). **E** Log2 abundance values for conventional EV and non-EV markers across all samples based on LC-MS/MS data. **F** Euler diagram comparing proteins from HD uEVs (≥ 50% detection), BlCa uEVs (≥ 50% detection), BlCa cell line EVs, and common protein signature (only including proteins found in tissue database). **G** Heatmap of log2-transformed abundances for proteins exclusive to BlCa patient uEVs and found across all cell line conditions and Dressler tissue database. Row annotations indicate subcellular localization and statistical significance

these proteins in uEVs from BlCa patients, using nine different publicly external datasets [32–40] of potential EV protein biomarker studies performed in BlCa urine samples and also using our own translational cohort. By crosschecking the common proteins with patient samples displayed in these databases (Supplementary Table 7), we identified 53 proteins in common with our study (Figure S8A). Moreover, six proteins – Heat Shock Protein 90 Alpha Family Class B Member 1 (HSP90AB1), Myristoylated alanine-rich C-kinase substrate (MARCKS), Annexin A1 (ANXA1), Annexin A2 (ANXA2), Nicotinamide phosphoribosyltransferase (NAMPT) and Myosin-9 (MYH9) – have been reported as upregulated in BlCa uEVs in more than one of these studies (Figure S8B). Additionally, we performed MS in a small translational cohort comprising six BlCa patients – ranging from in situ to muscle invasive disease – with age and gender matched HDs, to check if there were overlaps between our cell lines and proteins exclusively detected in BlCa patients. uEVs were successfully isolated as seen by the NTA profile and TEM images, showing no differences in particle concentration and mode size between cancer and healthy samples (Fig. 6A-D). Moreover, even though uromodulin (UMOD), which is the major urine protein contaminant, was found in uEVs, these samples also presented all the common EV markers (Fig. 6E).

Furthermore, EVs isolated from cell lines and urine were similar in size and common markers. Cell line-derived EVs ranged from 97 to 159 nm in mode, with an average of 126 nm, while urine-derived EVs displayed a range from 107 to 190 nm, presenting a similar average mode of 130 nm (Supplementary Tables 1 and 8). Molecularly, both EV sample types presented all common EV markers and largely lacked cellular contaminants.

When comparing BlCa cell line EVs, including the common proteins, with uEVs from BlCa and HDs, 408 proteins were present across the four groups, representing a high-confidence set of uEV proteins consistently expressed across patient samples, cell line models, and BlCa tissues (Fig. 6F). Nonetheless, each group presented exclusive proteins, with BlCa uEVs presenting 1,046 proteins not expressed in any other group. Notably, 52 out of the 486 proteins commonly expressed in BlCa cell lines and tissue data were also detected in urine from BlCa patients but absent from ≥ 50% of HD samples. Conversely, 613 BlCa cell line EV proteins were not detected in either urine groups, potentially reflecting differences between in vitro models and clinical specimens.

Interestingly, 13 proteins out of the 486 were found to be exclusive of BlCa uEVs (Fig. 6G). Scribble planar cell polarity protein (SCRIB), Transferrin receptor protein 1 (TFRC), Integrin alpha-2 (ITGA2), Integrin alpha-6 (ITGA6), Activated RNA polymerase II transcription factor 1 (SUB1), Minichromosome maintenance complex component 4 (MCM4), High mobility group box 2 (HMGB2), DEK proto-oncogene (DEK), Ribosomal protein L8 (RPL8), Ran GTPase activating protein 1 (RANGAP1), Serine and arginine rich splicing factor 1 (SRSF1), Serine and arginine rich splicing factor 2 (SRSF2) and Coiled-coil domain containing 47 (CCDC47) were present in at least half of the BlCa patient samples and absent from HDs. Additionally, ITGA2, ITGA6, SCRIB and TFRC were detected in all BlCa patient uEV samples, without being identified in any HDs and were also significantly upregulated (Figure S9 and Supplementary Table 9). These four proteins can be easily targeted since they are all located in the EV-membrane, demonstrating their potential as minimally invasive BlCa markers.

Discussion

The aim of this study was to uncover a core EV proteomic signature representative of the heterogenous nature of BlCa, specifically, the protein machinery driving disease biology and encapsulated within its secreted vesicles.

Advanced MS was performed to comprehensively characterize the proteomes of BlCa cell line-derived lysates and EVs across a broad disease spectrum. More importantly, following this discovery phase, we conducted retrospective validation of prioritized biomarkers using external datasets of differently expressed uEV proteins in BlCa patients, and a limited, valuable patient cohort to demonstrate their clinical relevance. To this end, uEV samples from BlCa patients and HDs were analyzed to assess the applicability of these markers in a real-world clinical setting.

BlCa encompasses extensive molecular and phenotypic heterogeneity, which is reflected in current molecular subtyping systems that distinguish groups such as luminal and basal, each carrying distinct clinical implications [41–45]. This diversity is mirrored in the included BlCa cell lines, that span from NMIBC and MIBC models and represent different stages, grades, and molecular subtypes. This strengthens the translational relevance of

proteins identified as part of the common EV signature. The variability observed across BlCa cell line EV profiles in this study is consistent with the broad biological spectrum of this malignancy and helps explain the complexity in finding BlCa-specific biomarkers. The fact that our study includes cell lines representative of this spectrum enabled the identification of a shared EV and lysate disease-specific signature across heterogeneity, rather than restricting analysis to subtype-specific patterns [46]. However, these subtype-specific EV profiles could also be important to be further explored, particularly in the context of tumor molecular stratification.

One major advantage of using cell lines is their capacity to provide virtually unlimited amounts of relevant biological material. This is particularly valuable for EV-focused studies, as EV yield from patient samples is often very low, making cell lines vital for early biomarker/therapeutic target discovery as well as cancer biology-related studies. Nonetheless, it is important to recognize that cell lines do not perfectly recapitulate tumors, especially due to intratumoral and interpatient heterogeneity, and tumor microenvironment complexity. Furthermore, although cell-derived EV collection parameters such as seeding density and viability assessment at the time of collection were standardized, some inter-replicate variability in EV secretion was observed across cell lines, which likely reflects intrinsic biological differences in EV biogenesis. Despite these limitations, in vitro models remain indispensable tools in EV and BlCa-related research.

Beyond simply identifying potential biomarkers, cell lines enable critical functional validation, demonstrating the relevant biological effects that EV cargo can exert on the tumor microenvironment and cancer metastasis [47]. This mechanistic insight is essential to confirm a biomarker's biological relevance rather than merely correlating with disease. Cell lines can also elucidate EV-mediated intercellular communication and identify targetable pathways that can be exploited therapeutically. Numerous BlCa cell line-EV studies have demonstrated that EV cargo can promote malignant phenotypes, with EVs from more aggressive cell lines influencing the behavior of less aggressive cells. These effects have been demonstrated across studies assessing proliferation, invasion, migration, drug resistance, and angiogenesis [48–55]. Hence, this proteomic signature offers a starting point for functional exploration of EV-mediated communication in BlCa, including the impact of specific EV proteins on BlCa spreading.

Given the inclusion of EVs from multiple sources, we employed a standardized differential UC protocol for EV isolation, enabling a controlled and source-independent EV proteomic content [24, 56]. The absence of a washing step may impair absolute purity and introduce some degree of co-isolation of non-EV particles and soluble proteins. However, UC-based washing has been shown to provide only marginal gains in purity while accounting for significant particle loss [57, 58]. Since none of the UC-based isolation methods currently offer optimal recovery regarding both EV yield and purity [27, 59, 60], we chose to maintain adequate recovery across two biofluids with distinct compositions, isolating EV populations with similar size across different biological sources. Another related challenge inherent to uEV proteomics is the co-isolation of UMOD, the most abundant protein in urine, which forms filamentous polymeric networks that co-sediment with uEVs during UC [61, 62]. In our study, UMOD was consistently detected across all uEV samples. This co-isolation is a well-recognized challenge across the majority of uEV enrichment methods, persisting even after more stringent isolation approaches [62]. While reducing agents such as dithiothreitol (DTT) or TCEP have been proposed to depolymerize UMOD, these treatments risk altering the structure of disulfide bond-dependent proteins and do not fully prevent co-sedimentation upon UC. Moreover, its ubiquitous presence even in the most rigorous isolation approaches suggests that it may also represent a legitimate uEV cargo protein carried by a subset of uEVs, and complete removal is not always achievable or even desirable depending on the study focus [62]. Overall, our study design adhered to MISEV guidelines, which is essential to minimize methodological variability in EV research [27], and patient-derived samples were collected and processed using a routine standard operating procedure to mitigate pre-analytical variability. This is a known significant challenge in liquid biopsy studies [63], strengthening the translational relevance of the resulting signatures.

In our study, proteome analysis shows distinct profiles between EVs and lysates. Low correlation and inter-cell-line variability between EV and parental cell proteomes has been previously documented [64, 65], with small EVs exhibiting significantly lower protein correlation with intracellular levels compared to non-vesicular fractions [66]. Collectively, these findings establish that low and variable EV-to-cell proteome correlation is biologically meaningful, reflecting active cargo selection mechanisms rather than a technical artefact. Moreover, correlation strength of lysates with their derived EVs and other cell lines' EVs was not significantly different, suggesting that vesicle-associated information is similar across cell lines. Interestingly, lysate proteomic profile formed two different clusters, one comprising less aggressive cell lines (SW780, RT112 and J82) and another consisting of more aggressive and metastatic models (UMUC3, 253 J and T24). Although J82 originates from a high-grade (G3), pT3 tumor, and is generally considered aggressive, previous reports show that it shares several features with less

aggressive, luminal, or papillary cell lines such as SW780 and RT112, rather than clustering with highly mesenchymal or more aggressive cell lines such as UMUC3, T24 or 253 J [21, 22, 28]. In contrast, EVs showed similarities across conditions, suggesting once again that EV cargo appears largely cell-line independent, consistent with previous studies [65].

As expected, lysates presented a higher number of unique proteins than EVs: among the 6,613 proteins identified across all replicates in at least one condition, lysates comprised roughly 5,000 proteins, whereas EVs contained approximately 2,000 distinct proteins. Furthermore, we compared proteins identified in this study with external public databases, and most listed proteins were also present in our dataset, reinforcing the robustness and reliability of our results [29, 30]. Importantly, a substantial fraction of the proteins identified here represent novel data, thereby expanding the current proteomic landscape.

To reach a protein signature shared across all lysates and EVs derived from all BlCa cell lines, we stratified our dataset into three groups: proteins common to both lysates and EVs, lysate-exclusive proteins, and EV-exclusive proteins. This analysis showed that these three groups differed markedly in protein abundance, subcellular localization and biological functions. It should also be noted that subcellular compartment classifications and biological processes reflect the known properties of each protein in the producing cell, rather than its physical localization or biological function within the EV itself. To further understand these proteins' location in the EVs and its implication on specific biological mechanisms, dedicated approaches such as proteinase K protection assays or surface biotinylation strategies should be further explored [67–70]. Nonetheless, common proteins were primarily associated with proliferation and migration, whereas lysate-exclusive proteins were enriched in pathways related to energy production, and EV-exclusive proteins were linked to hemostasis and defense responses, highlighting the functional diversity of these proteomic subsets. Additionally, we show that only 25% of the proteomic profile of lysates and EVs is shared, and this overlap is consistent across the different cell lines. Lysates retain most of their protein content without packaging it into EVs, which is justified by the localization of these proteins, since they are mainly associated with the nucleus and mitochondria, a feature that is not present in EV biogenesis [27, 71]. In contrast, most proteins present in EVs were shared with the lysate's proteome, confirming that EVs do mimic their cell of origin.

Since our purpose was to identify a common BlCa signature with potential translational value, we evaluated whether our proteins reflected those found in patient-derived bladder tissues, covering the full spectrum of BlCa lesions, from Dressler and colleagues. Using this dataset for comparison, we observed that more than 5,000 of the 6,613 proteins identified in our study were also present in BlCa patients' tissues. This finding shows that both lysates and EVs from BlCa in vitro models highly mimic what is expressed in patient samples, addressing their clinical utility and suggesting its translational potential. Approximately 30% of tissue proteins, however, were not detected in our dataset. This discrepancy likely reflects the contribution of tumor microenvironment to tissue proteomic diversity [72, 73], as tissue fragments contain not only tumor cells but also stromal, immune, and vascular components, which are not captured in monoculture models. Focusing specifically on the 497 proteins shared across all cell lines and EVs, only 11 were absent from the tissue proteomics dataset. This high degree of overlap underscores the biological relevance of the shared proteomic signature and suggests that, despite their simplified nature, BlCa cell lines capture key clinically important molecular features of the disease.

The translational potential of this signature was further evaluated in uEVs from BlCa patients and HDs, both in external datasets and in a small translational cohort. The use of cell line–derived EVs and patient uEVs represent complementary but distinct experimental contexts. Despite these differences, previous studies have demonstrated meaningful overlap between cell line EVs and patient-derived uEVs proteomes [51, 74] and transcriptomes [46], supporting the translational relevance of cell line–based discovery strategies. Altogether, these observations support our study design, in which cell line–derived EV proteomics serves as a controlled discovery platform, with translational relevance assessed through cross-comparison with patient uEV data. Urine represents the ideal source of non-invasive BlCa biomarkers, since it maintains direct contact with bladder tumor cells. For EV focused studies, this is particularly advantageous, as urine becomes enriched in tumor-derived EVs while minimizing contamination from EVs originating from non-urological tissue [75].

To further assess this translational robustness, we performed a systematic cross-study comparison of our cell line-derived signature against nine published BlCa uEV proteomic datasets, focusing on proteins reported as upregulated in BlCa patients. This analysis identified 53 candidate proteins with prior independent evidence of BlCa-associated detection in patient uEVs across multiple studies, with six proteins detected in more than one independent cohort. Notably, proteins unveiled in multiple independent datasets represent the most translationally consistent candidates, being identified across distinct patient populations, isolation protocols, and analytical platforms. This cross-study convergence substantially

Table 3 List of uEV proteins and their roles in cancer, BlCa, EVs and BlCa-derived EVs with respective protein reported studies. ALT: alternative lengthening of telomeres, CNS: Central nervous system, ECM: Extracellular matrix, EMT: Epithelial mesenchymal transition, HGSOC: High grade serous ovarian carcinoma, NR: Not reported

Protein	Function Role in cancer	BlCa	General EVs	BlCa-EV
SCRIB	Involved in cell polarity, tumor suppressor [77]	Polarity disruption during urothelial carcinoma progression/EMT involvement [78]	NR	NR
TFRC	Iron metabolism and cell proliferation [79, 80]	Diagnostic marker, with higher expression in tumor tissues [81] and as therapeutic targets [82]	First EV identified protein [83, 84], potential nanocarriers for CNS parenchyma [85]	NR
ITGA2	ECM adhesion, promotes EMT, invasion and migration [86, 87]	Cell proliferation, migration, and tumorigenesis [88]	HGSOC[89], lung cancer [90], pancreatic cancer [91]	NR
ITGA6	Laminin-binding integrin, cell adhesion, lymphangiogenesis, metastasis	Higher expression of ITGA6 correlated with poor prognosis [92]	Metastasis promotion in ovarian and pancreatic cancer [93, 94]	Tissue derived EVs: pre-metastatic niche in draining lymph nodes [76]
SUB1	Transcriptional co-activator and chromatin regulator. ALT, genome stability [95]	Elevated in BlCa, associated with survival, related with cancer stemness genes, potential therapy target [96]	NR	NR
MCM4	DNA replication, uncontrolled proliferation [97, 98]	Overexpressed in BlCa cell lines [28], MCM family protein overexpressed across stages [31, 99]	NR	NR
HMGB2	Increases DNA repair efficiency, radioresistance [100, 101]	Associated with progression and angiogenesis [102]	Muscle cell-EVs [103], plasma EVs [104]	NR
DEK	Affects DNA damage repair; proliferation; inhibits apoptosis [105]	BlCa tissues and urine [106]	NR	NR
RPL8	Proliferation via transcriptome and ALT [107]	NR	NR	NR
RANGAP1	Nuclear protein export, pro-oncogenic [108]	NR	Nuclear export signal-cargo in sEVs [109]	NR
SRSF1	Alters splicing of crucial cell cycle regulatory genes and tumor suppressors, oncoprotein [110]	Cell growth and migration [111], poor prognosis and cisplatin resistance [112]	Cell line derived and plasma-derived EVs [113]	NR
SRSF2	Pre-mRNA splicing/AS [110]	Repressed in chemoresistance [114]	Cell line derived and plasma-derived EVs [113]	NR
CCDC47	ER protein folding, calcium signaling [115]	NR	NR	NR

strengthens the translational relevance of our signature and provides an external, multi-cohort framework.

Interestingly, from the 486 identified targets in all cell lines and present in BlCa tissues, 460 were present in urine, reflecting their translation to human samples. 13 were exclusively present in uEVs of BlCa patients, four of which (ITGA2, ITGA6, SCRIB and TFRC) were also significantly upregulated and consistently detected across all BlCa samples analyzed.

Six out of 13 identified proteins have been implicated in BlCa or EV biology, however, the only protein documented and explored in BlCa-derived EVs was ITGA6 (Table 3). Also by an MS approach, Lin et al. identified and studied the role of BlCa tissue derived ITGA6+-EVs. These EVs targeted lymphatic vessels through ITGA6-CD151 interplay and released *circRNA-LIPAR* to induce E-selectin (SELE) overexpression. Moreover, by engineering ITGA6+-EVs, lymphatic metastasis was suppressed and survival rates increased, suggesting a clear therapeutic application [76]. Our study adds another layer to the importance of this marker by detecting ITGA6 in a different EV source – urine. This suggests that the importance of ITGA6-EVs extends beyond local tissue to systemic release. Therefore, further exploration of the other 12 identified proteins in BlCa-EVs has the potential to enhance our knowledge regarding the relevance of these targets for BlCa detection and therapeutic management.

Independent omics studies collectively point towards a consistent biological portrait of BlCa EVs, supporting the existence of a disease-associated EV molecular signature from cell-of-origin to EV. Our findings align and extend with recent RNA and glycan studies performed in BlCa EVs [46, 116]. Sun and colleagues demonstrated

that BlCa cell line–derived EV-mRNA profiles can be translated to patient uEVs and support the concept of a "core BlCa EV transcriptome" with strong diagnostic performance. Likewise, N-glycomics of BlCa patients' uEVs have revealed disease-associated EV N-glycan patterns, some of which are conserved across BlCa cell lines and patient samples. In line with these findings, we observed a similar pattern at the protein level, further supporting that EV cargo captures overlapping intrinsic characteristics of BlCa biology. Indeed, this work adds a comprehensive protein-level dimension to this emerging picture, defining a BlCa cell line–derived EV proteomic signature that is detectable in tumor tissue and mirrored, at least in part, in uEVs from patients.

To the best of our knowledge, this is the first comprehensive proteomic study in BlCa EVs across a broad panel of in vitro models spanning relevant disease stages and phenotypes. This study provides a proof-of-concept for the utility of the EV proteome as a source of novel biomarkers in BlCa, as well as targets for functional studies and new potential therapeutic interventions. Our strategy to progress from cell lines to patient-derived samples, supported by external tissue and uEV proteomics data and validation in biofluids, demonstrates the feasibility of translating in vitro findings into clinically relevant applications and enables rational prioritization of candidates for translation.

Nonetheless, study limitations must be acknowledged. One limitation of this study is the absence of a non-cancerous bladder cell line as an in vitro reference. Truly "normal" urothelial cell lines are hampered by the effects of immortalization, which irrespectively of the method employed, even for the least disruptive approaches, introduces significant genetic and functional alterations that compromise normal urothelial biology [117, 118]. In order to overcome this hurdle, uEVs from HDs were used as the non-cancer comparator, reflecting the in vivo urothelial milieu in a physiologically meaningful way. Future studies incorporating the use of different primary normal human urothelial (NHU) cell cultures or patient-derived organoids [119] may offer improved biological relevance over immortalized cell line models for EV studies. The addition of HD samples provided a cancer-associated signature to our candidate proteins. However, the inclusion of additional control groups, such as patients with benign urological conditions including urinary tract infections, benign prostatic hyperplasia, or nephrolithiasis, as well as inflammatory disorders and other urological malignancies, could be useful to establish a more solid clinical BlCa-specific signature.

One of our primary aims was to establish the translational potential of our findings through comparison with published uEV studies and direct MS analysis of patient samples. Thus, validation of the most promising candidates by targeted immunoassays or antibody-based approaches in a larger cohort remains an important next step to confirm the observed trends and assess their robustness. Nevertheless, LC-MS/MS-based proteomics is increasingly recognized as a powerful tool for cancer biomarker detection in its own right, offering advantages over conventional immunoassays, including multiplexing capacity and analytical specificity [120–123]. MS-based analysis of biofluids is an emerging and rapidly advancing area with growing clinical translation potential [124, 125], and targeted MS approaches such as multiple reaction monitoring and parallel reaction monitoring are actively being developed as clinical-grade oncology assays [126]. The candidate panel identified here is therefore well-positioned for further development within both immunoassay-based and targeted MS-driven clinical validation frameworks.

Our identified protein signature has the potential to be further explored: (1) functionally, to understand the role of these proteins in BlCa EV-mediated tumor communication; (2) in BlCa-enriched EV isolation strategies, particularly as some targets, such as integrins and SCRIB, are transmembrane proteins that, through high-throughput techniques such as microfluidics devices, could enable targeted capture or detection of BlCa EVs [127–129]; and (3) in exploration of therapeutic strategies aimed at modulating the expression of these proteins.

Overall, we identified a common EV-derived proteomic signature spanning diverse BlCa stages and demonstrated its translational potential to ultimately improve disease diagnosis and management for better patient outcomes.

Supplementary Information

The online version contains supplementary material available at https://doi.org/10.1186/s12964-026-02868-2.

Supplementary Material 1: Figure S1 – Characterization of BlCa cell lines and derived EVs. (A) Representative phase-contrast microscope images of BlCa cell lines (upper panel) and transmission electron microscope and derived EVs (lower panel). (B) EV mean size distribution and (C) particle number per mL across the different cell lines. Statistical analysis was performed using the Kruskal-Wallis test, *$p<0.05$, **$p<0.01$. Results are presented as mean ± SEM. Figure S2 – BlCa cell line proteomics filtering criteria. Figure S3 – Euler diagrams showing total number and percentage overlap and exclusivity from lysate and EV from each individual cell line. Figure S4 – BlCa cell line derived-EV particle and proteomic characterization. (A) Bar plot of individual protein number detected by LC-MS/MS across all BlCa cell line lysate and EV replicates. (B) Boxplot showing the median number of proteins detected by LC-MS/MS across conditions. Figure S5 – Validation of BlCa cell line derived proteins in external datasets. (A) Euler diagram crosschecking this study lysate proteins with another BlCa cell line lysate proteomic study. Venn diagram representing overlap of this study EV proteins with two external databases, Exocarta and Vesiclepedia, for (B) the Top 100 most common protein lists, and (C) BlCa cell line derived EVs lists. Figure S6 – Proteomic characterization of common proteins. (A) Hierarchical clustering of Pearson correlations among all replicates. (B) Comparison between this study common proteins and BlCa cell line-derived EVs from Vesiclepedia and Exocarta. Figure S7 – Enrichment analysis of the different BlCa cell lines datasets. Bar plots of enriched GO Biological Process terms for Common (up), EV- (middle) and Lysate-exclusive proteins (bottom).

Figure S8 – Literature uEV validation of common BlCa cell line signature. (A) Euler diagram showing overlap between proteins common to all cell line conditions and upregulated proteins from published uEV studies. (B) Network visualization of protein-study associations. Protein nodes are colored by category: orange nodes are common cell line proteins present in multi-studies and blue represent the literature studies. Node size reflects number of connections. Figure S9 – Individual protein abundance comparison between BlCa patients and HDs in uEVs. Boxplots showing log2-transformed protein abundance for each of the 13 proteins identified as BlCa-exclusive (detected in ≥3 BlCa samples and 0 HD samples) and overlapping with the cell line EV proteome signature. Statistical significance was determined using the Wilcoxon rank-sum test: $^{**}p < 0.01$, ns = not significant.

Supplementary Material 2: Supplementary Table 1 – BlCa cell line culture measurements and NTA values of derived-EVs. Supplementary Table 2 – Pearson correlations between matched lysate and EVs across all proteins. Supplementary Table 3 – Numbers and percentages of proteins exclusive and overlapping in each cell line. Supplementary Tables 4 – Composition of lysate and EV proteomes. Supplementary Tables 5 – Number of present proteins in each BlCa condition. Supplementary Tables 6 – Pearson correlations between matched lysate and EVs across common proteins. Supplementary Tables 7 – Proteomic datasets of BlCa patient uEV studies. Supplementary Tables 8 – uEV NTA values. Supplementary Tables 9 – Wilcoxon Results. Supplementary Tables 10 – Sample nomenclature.

Acknowledgements
The authors are grateful to the Department of Pathology & Laboratory Medicine for their collaboration in sample collection. We thank the HEMS and to Hugo Osorio from Proteomics scientific platforms at i3S for TEM image acquisition and the mass spectrometry analysis, respectively. The authors would like to extend their appreciation to all the patients and control subjects who kindly provided the biological samples for this study.

Authors' contributions
CL, AC and CJ conceived and designed the study. CL and NTT performed the experiments. CL and VC performed the bioinformatic analyses. CL analyzed the data and drafted the manuscript. VC, SMR and JL provided scientific input and guidance throughout the project. RSS provided help with liquid biopsy processing. JL performed pathological revision and provided clinical information about the patients. AC and CJ supervised the research project. All authors revised and approved the manuscript.

Funding
This study is funded by Fundaçao para a Ciência e Tecnologia (FCT) (DOI: https://doi.org/10.54499/2023.16683.ICDT) and the IPO Porto Research Center R&D funding (DOI: https://doi.org/10.54499/UID/00776/2025). Additional funding of GEBC: PI 27-CI- IPOP-27-2016 and EMBRACIVE PI 224-CI-IPOP-74-2024. VC is a postdoc fellow under PROMISE project (https://doi.org/10.54499/2023.16683.ICDT). CL and NTT hold PhD fellowships from FCT by projects 2021.06731.BD and 2022.09566.BD, respectively (DOI: https://doi.org/10.54499/2021.06731.BD and DOI: https://doi.org/10.54499/2022.09566.BD).

Data availability
All MS proteomics data have been deposited to the ProteomeXchange Consortium via the PRIDE partner repository. BlCa cell line datasets are under the PXD071837 identifier and PXD062618 corresponds to the uEV proteomics data.

Declarations

Ethics approval and consent to participate
Samples were collected after obtaining patient informed consent and ethics approval (CES 174/022).

Consent for publication
Not applicable.

Competing interests
The authors declare no competing interests.

Author details
[1]Cancer Biology & Epigenetics Group, IPO Porto Research Center (CI-IPOP), Portuguese Oncology Institute of Porto (IPO Porto), Porto, Portugal
[2]CI-IPOP @ RISE-Associated Laboratory and Porto Comprehensive Cancer Center Raquel Seruca (Porto.CCC), R. Dr. António Bernardino de Almeida, Porto, Portugal
[3]Doctoral Programme in Biomedical Sciences, ICBAS-School Medicine and Biomedical Sciences- University of Porto, Porto, Portugal
[4]i3S-Instituto de Investigação e Inovação em Saúde – Universidade do Porto, Porto, Portugal
[5]Department of Pathology, Portuguese Oncology Institute of Porto, Porto, Portugal
[6]BBIT Therapeutics, Porto, Portugal
[7]Department of Pathology and Molecular Immunology, ICBAS- School of Medicine & Biomedical Sciences- University of Porto, Porto, Portugal

Received: 15 December 2025 / Accepted: 29 March 2026
Published online: 09 April 2026

References

1. Bray FA-O et al. Global cancer statistics 2022: GLOBOCAN estimates of incidence and mortality worldwide for 36 cancers in 185 countries.CA Cancer J Clin. 2024;74(3):229–263..
2. Zhang Y, et al. The global landscape of bladder cancer incidence and mortality in 2020 and projections to 2040. J Glob Health. 2023;13:04109.
3. Dyrskjøt L, et al. Bladder cancer. Nat Rev Dis Primers. 2023;9(1):58.
4. Grabe-Heyne K, et al. Intermediate and high-risk non-muscle-invasive bladder cancer: an overview of epidemiology, burden, and unmet needs. Front Oncol. 2023;13:1170124.
5. Holzbeierlein J, et al. Treatment of Non-Metastatic Muscle-Invasive Bladder Cancer: AUA/ASCO/SUO Guideline (2017; Amended 2020, 2024). J Urol. 2024;212(1):3–10.
6. Ahangar M, Mahjoubi F, Mowla SJ. Bladder cancer biomarkers: current approaches and future directions. Front Oncol. 2024;14:1453278.
7. Zhu CZ, et al. A review on the accuracy of bladder cancer detection methods. J Cancer. 2019;10(17):4038–44.
8. Godlewski D, et al. Bladder cancer biomarkers. Explor Target Antitumor Ther. 2025;6:1002301.
9. Devlies W, et al. The Diagnostic Accuracy of Cystoscopy for Detecting Bladder Cancer in Adults Presenting with Haematuria: A Systematic Review from the European Association of Urology Guidelines Office. Eur Urol Focus. 2024;10(1):115–22.
10. Sievert KD, et al. Economic aspects of bladder cancer: what are the benefits and costs? World J Urol. 2009;27(3):295–300.
11. Liu YJ, Wang C. A review of the regulatory mechanisms of extracellular vesicles-mediated intercellular communication. Cell Commun Signal. 2023;21(1):77.
12. Greening DW, et al. Clinical relevance of extracellular vesicles in cancer - therapeutic and diagnostic potential. Nat Rev Clin Oncol. 2025;22(12):924–52.
13. Bandu R, Oh JW, Kim KP. Mass spectrometry-based proteome profiling of extracellular vesicles and their roles in cancer biology. Exp Mol Med. 2019;51(3):1–10.
14. Murakami T, et al. Cross-sectional and longitudinal analyses of urinary extracellular vesicle mRNA markers in urothelial bladder cancer patients. Sci Rep. 2024;14(1):6801.
15. Wang S, et al. Tumor-derived extracellular vesicles modulate innate immune responses to affect tumor progression. Front Immunol. 2022;13:1045624.
16. Rodríguez-Cobos J et al. ΔNp73, TAp73 and Δ133p53 extracellular vesicle cargo as Early diagnosis markers in colorectal cancer. Cancers (Basel). 2021;13(9):2240.
17. Witwer KW et al. Standardization of sample collection, isolation and analysis methods in extracellular vesicle research. J Extracell Vesicles. 2013;2(1).
18. Rontogianni S, et al. Proteomic profiling of extracellular vesicles allows for human breast cancer subtyping. Commun Biol. 2019;2:325.
19. Dalla PV et al. Selectively-Packaged Proteins in Breast Cancer Extracellular Vesicles Involved in Metastasis. Int J Mol Sci, 2020;21(14):4990.
20. Ju J, et al. Extracellular vesicles: cargo loading, degradation and secretory pathways, and their intersection with autophagy. Extracell Vesicles Circ Nucl Acids. 2025;6(3):360–85.

21. Warrick JI, et al. FOXA1, GATA3 and PPARɣ Cooperate to Drive Luminal Subtype in Bladder Cancer: A Molecular Analysis of Established Human Cell Lines. Sci Rep. 2016;6:38531.
22. Eray A, Erkek-Özhan S. Classification of bladder cancer cell lines according to regulon activity. Turk J Biol. 2021;45(6):656–66.
23. Zuiverloon TCM, et al. Systematic Review: Characteristics and Preclinical Uses of Bladder Cancer Cell Lines. Bladder Cancer. 2018;4(2):169–83.
24. Hoshino A, et al. Extracellular Vesicle and Particle Biomarkers Define Multiple Human Cancers. Cell. 2020;182(4):1044–e106118.
25. Tavares NT, et al. MicroRNA-371-373 cluster extracellular vesicle-based communication in testicular germ cell tumors. Cell Commun Signal. 2025;23(1):252.
26. Osório H et al. Proteomics Analysis of Gastric Cancer Patients with Diabetes Mellitus. J Clin Med, 2021;10(3):407.
27. Welsh JA, et al. Minimal information for studies of extracellular vesicles (MISEV2023): From basic to advanced approaches. J Extracell Vesicles. 2024;13(2):e12404.
28. Puttamallesh VN et al. Quantitative Proteomics of Urinary Bladder Cancer Cell Lines Identify UAP1 as a Potential Therapeutic Target. Genes (Basel). 2020;11(7).
29. Keerthikumar S, et al. ExoCarta: A Web-Based Compendium of Exosomal Cargo. J Mol Biol. 2016;428(4):688–92.
30. Chitti SV, et al. Vesiclepedia 2024: an extracellular vesicles and extracellular particles repository. Nucleic Acids Res. 2024;52(D1):D1694–8.
31. Dressler FF, et al. Proteomic analysis of the urothelial cancer landscape. Nat Commun. 2024;15(1):4513.
32. Suh J, et al. Next-generation Proteomics-Based Discovery, Verification, and Validation of Urine Biomarkers for Bladder Cancer Diagnosis. Cancer Res Treat. 2022;54(3):882–93.
33. Zhou X, et al. Exploration of potential biomarkers for early bladder cancer based on urine proteomics. Front Oncol. 2024;14:1309842.
34. Tomiyama E, et al. Proteomic analysis of urinary and tissue-exudative extracellular vesicles to discover novel bladder cancer biomarkers. Cancer Sci. 2021;112(5):2033–45.
35. Lee J, et al. Altered Proteome of Extracellular Vesicles Derived from Bladder Cancer Patients Urine. Mol Cells. 2018;41(3):179–87.
36. Hiltbrunner S, et al. Urinary Exosomes from Bladder Cancer Patients Show a Residual Cancer Phenotype despite Complete Pathological Downstaging. Sci Rep. 2020;10(1):5960.
37. Jordaens S et al. Protein Biomarker Discovery Studies on Urinary sEV Fractions Separated with UF-SEC for the First Diagnosis and Detection of Recurrence in Bladder Cancer Patients. Biomolecules. 2023;13(6):932.
38. Igami K, et al. Extracellular vesicles expressing CEACAM proteins in the urine of bladder cancer patients. Cancer Sci. 2022;113(9):3120–33.
39. Lin SY, et al. Proteome Profiling of Urinary Exosomes Identifies Alpha 1-Antitrypsin and H2B1K as Diagnostic and Prognostic Biomarkers for Urothelial Carcinoma. Sci Rep. 2016;6:34446.
40. Chen CL, et al. Comparative and targeted proteomic analyses of urinary microparticles from bladder cancer and hernia patients. J Proteome Res. 2012;11(12):5611–29.
41. The Cancer Genome Atlas Research Network. Comprehensive molecular characterization of urothelial bladder carcinoma. Nature. 2014;507(7492):315–22.
42. Kamoun A, et al. A Consensus Molecular Classification of Muscle-invasive Bladder Cancer. Eur Urol. 2020;77(4):420–33.
43. Sjödahl G, et al. Different Responses to Neoadjuvant Chemotherapy in Urothelial Carcinoma Molecular Subtypes. Eur Urol. 2022;81(5):523–32.
44. Robertson AG, et al. Comprehensive Molecular Characterization of Muscle-Invasive Bladder Cancer. Cell. 2017;171(3):540–e55625.
45. Guo CC, et al. Molecular profile of bladder cancer progression to clinically aggressive subtypes. Nat Rev Urol. 2024;21(7):391–405.
46. Sun N, et al. Unveiling urinary extracellular vesicle mRNA signature for early diagnosis and prognosis of bladder cancer. Theranostics. 2025;15(4):1272–84.
47. Xu K, et al. Elevated extracellular matrix protein 1 in circulating extracellular vesicles supports breast cancer progression under obesity conditions. Nat Commun. 2024;15(1):1685.
48. Boddu VK, et al. Targeting cancer-derived extracellular vesicles by combining CD147 inhibition with tissue factor pathway inhibitor for the management of urothelial cancer cells. Cell Commun Signal. 2024;22(1):129.
49. Prieto-Vila M, et al. High-grade bladder cancer cells secrete extracellular vesicles containing miRNA-146a-5p and promotes angiogenesis. J Extracell Biol. 2022;1(8):e47.
50. Yang L, et al. Bladder cancer cell-derived exosomes inhibit tumor cell apoptosis and induce cell proliferation in vitro. Mol Med Rep. 2013;8(4):1272–8.
51. Silvers CR, et al. Identification of extracellular vesicle-borne periostin as a feature of muscle-invasive bladder cancer. Oncotarget. 2016;7(17):23335–45.
52. Ostenfeld MS, et al. Cellular disposal of miR23b by RAB27-dependent exosome release is linked to acquisition of metastatic properties. Cancer Res. 2014;74(20):5758–71.
53. Beckham CJ, et al. Bladder cancer exosomes contain EDIL-3/Del1 and facilitate cancer progression. J Urol. 2014;192(2):583–92.
54. Franzen CA, et al. Urothelial cells undergo epithelial-to-mesenchymal transition after exposure to muscle invasive bladder cancer exosomes. Oncogenesis. 2015;4(8):e163–163.
55. Ringuette Goulet C, et al. Exosomes Induce Fibroblast Differentiation into Cancer-Associated Fibroblasts through TGFβ Signaling. Mol Cancer Res. 2018;16(7):1196–204.
56. Lourenço C et al. Urinary extracellular vesicles as potential biomarkers for urologic cancers: an overview of current methods and advances. Cancers (Basel). 2021;13(7):1529.
57. Webber J, Clayton A. How pure are your vesicles? Journal of Extracellular Vesicles, 2013;2(1).
58. Teixeira-Marques A, et al. Improved recovery of urinary small extracellular vesicles by differential ultracentrifugation. Sci Rep. 2024;14(1):12267.
59. Williams S, et al. Comparison of extracellular vesicle isolation processes for therapeutic applications. J Tissue Eng. 2023;14:20417314231174609.
60. Zhao Z, et al. Isolation and analysis methods of extracellular vesicles (EVs). Extracell Vesicles Circ Nucl Acids. 2021;2(1):80–103.
61. Erdbrügger U, et al. Urinary extracellular vesicles: A position paper by the Urine Task Force of the International Society for Extracellular Vesicles. J Extracell Vesicles. 2021;10(7):e12093.
62. Harding MA, et al. Uromodulin and the study of urinary extracellular vesicles. J Extracell Biol. 2024;3(11):e70022.
63. Batool SM, et al. Extrinsic and intrinsic preanalytical variables affecting liquid biopsy in cancer. Cell Rep Med. 2023;4(10):101196.
64. Luo HT, et al. Dissecting the multi-omics atlas of the exosomes released by human lung adenocarcinoma stem-like cells. NPJ Genom Med. 2021;6(1):48.
65. Hurwitz SN, et al. Proteomic profiling of NCI-60 extracellular vesicles uncovers common protein cargo and cancer type-specific biomarkers. Oncotarget. 2016;7(52):86999–7015.
66. Morales-Sanfrutos J et al. Defining the reference proteomes for small extracellular vesicles and non-vesicular components. Nat Cell Biol. 2026;28(3):622–39.
67. Cvjetkovic A, et al. Detailed Analysis of Protein Topology of Extracellular Vesicles-Evidence of Unconventional Membrane Protein Orientation. Sci Rep. 2016;6:36338.
68. Kirkemo LL et al. Cell-surface tethered promiscuous biotinylators enable comparative small-scale surface proteomic analysis of human extracellular vesicles and cells. Elife. 2022;11:e73982
69. Rai A, et al. Proteomic dissection of large extracellular vesicle surfaceome unravels interactive surface platform. J Extracell Vesicles. 2021;10(13):e12164.
70. Fochtman D, et al. Challenges of MS-based small extracellular vesicles proteomics. J Extracell Vesicles. 2024;13(12):e70020.
71. Mulcahy LA, Pink RC, Carter DR. Routes and mechanisms of extracellular vesicle uptake. J Extracell Vesicles. 2014;3(1):24641.
72. Hong Z, et al. Proteomic Profiling and Tumor Microenvironment Characterization Reveal Molecular and Immunological Hallmarks of Left-Sided and Right-Sided Colon Cancer Tumorigenesis. J Proteome Res. 2023;22(9):2973–84.
73. Hanash S, Schliekelman M. Proteomic profiling of the tumor microenvironment: recent insights and the search for biomarkers. Genome Med. 2014;6(2):12.
74. Welton JL, et al. Proteomics analysis of bladder cancer exosomes. Mol Cell Proteom. 2010;9(6):1324–38.
75. Oliveira MC et al. Urinary Biomarkers in Bladder Cancer: Where Do We Stand and Potential Role of Extracellular Vesicles. Cancers (Basel). 2020;12(6):1400.
76. Lin Y, et al. Integrin α6-containing extracellular vesicles promote lymphatic remodelling for pre-metastatic niche formation in lymph nodes via interplay with CD151. J Extracell Vesicles. 2024;13(10):e12518.
77. Kapil S, et al. The cell polarity protein Scrib functions as a tumor suppressor in liver cancer. Oncotarget. 2017;8(16):26515–31.
78. Namdarian B, et al. Loss of APKC expression independently predicts tumor recurrence in superficial bladder cancers. Urol Oncol. 2013;31(5):649–55.
79. Kim H, et al. Transferrin Receptor-Mediated Iron Uptake Promotes Colon Tumorigenesis. Adv Sci (Weinh). 2023;10(10):e2207693.

80. Ren G, et al. TFRC promotes the proliferation, migration, and invasion of osteosarcoma cells by increasing the intracellular iron content and RRM2 expression. Front Oncol. 2025;15:1567216.
81. Qin J, et al. Expression of transferrin receptor/TFRC protein in bladder cancer cell T24 and its role in inducing iron death in bladder cancer. Int J Biol Macromol. 2024;274(Pt 1):133323.
82. Bahrami S, et al. Discovering Therapeutic Protein Targets for Bladder Cancer Using Proteomic Data Analysis. Curr Mol Pharmacol. 2020;13(2):150–72.
83. Johnstone RM, et al. Vesicle formation during reticulocyte maturation. Association of plasma membrane activities with released vesicles (exosomes). J Biol Chem. 1987;262(19):9412–20.
84. Gardner JO, et al. LC3-dependent EV loading and secretion (LDELS) promotes TFRC (transferrin receptor) secretion via extracellular vesicles. Autophagy. 2023;19(5):1551–61.
85. Mattera VS, et al. Extracellular vesicles containing the transferrin receptor as nanocarriers of apotransferrin. J Neurochem. 2020;155(3):327–38.
86. Rattanasinchai C, Navasumrit P, Ruchirawat M. Elevated ITGA2 expression promotes collagen type I-induced clonogenic growth of intrahepatic cholangiocarcinoma. Sci Rep. 2022;12(1):22429.
87. Arun AS, Tepper CG, Lam KS. Identification of integrin drug targets for 17 solid tumor types. Oncotarget. 2018;9(53):30146–62.
88. Dai R, et al. Lnc-STYK1-2 regulates bladder cancer cell proliferation, migration, and invasion by targeting miR-146b-5p expression and AKT/STAT3/NF-kB signaling. Cancer Cell Int. 2021;21(1):408.
89. Trinidad CV, et al. Lineage specific extracellular vesicle-associated protein biomarkers for the early detection of high grade serous ovarian cancer. Sci Rep. 2023;13(1):18341.
90. Ruzycka-Ayoush M et al. Extracellular vesicles as next-generation biomarkers in lung cancer patients: a case report on adenocarcinoma and squamous cell carcinoma. Life (Basel). 2024;14(3).
91. Ferrara B, et al. Matrix stiffness regulates the protein profile of extracellular vesicles of pancreatic cancer cell lines. Proteomics. 2024;24(23–24):e2400058.
92. Jin H, et al. N(6)-methyladenosine modification of ITGA6 mRNA promotes the development and progression of bladder cancer. EBioMedicine. 2019;47:195–207.
93. Gambelli A, et al. Author Correction: Platinum-induced upregulation of ITGA6 promotes chemoresistance and spreading in ovarian cancer. EMBO Mol Med. 2024;16(8):1981.
94. Wu Y, et al. ITGA6 and RPSA synergistically promote pancreatic cancer invasion and metastasis via PI3K and MAPK signaling pathways. Exp Cell Res. 2019;379(1):30–47.
95. Dubois JC, et al. The single-stranded DNA-binding factor SUB1/PC4 alleviates replication stress at telomeres and is a vulnerability of ALT cancer cells. Proc Natl Acad Sci U S A. 2025;122(2):e2419712122.
96. Yan B, et al. PC4 promotes bladder cancer progression and stemness by directly interacting with Sp1 to transcriptionally activate the Wnt5a/β-catenin pathway. Pathol Res Pract. 2024;259:155369.
97. Tan Y, Ding L, Li G. MCM4 acts as a biomarker for LUAD prognosis. J Cell Mol Med. 2023;27(21):3354–62.
98. Yang S, et al. MCM4 is a novel prognostic biomarker and promotes cancer cell growth in glioma. Front Oncol. 2022;12:1004324.
99. Korkolopoulou P, et al. Minichromosome maintenance proteins 2 and 5 expression in muscle-invasive urothelial cancer: a multivariate survival study including proliferation markers and cell cycle regulators. Hum Pathol. 2005;36(8):899–907.
100. Zhu Y, et al. Predictive and clinicopathological importance of HMGB2 in various carcinomas: a meta and bioinformatic approach. Sci Rep. 2025;15(1):11003.
101. Shin YJ, et al. High-mobility group box 2 (HMGB2) modulates radioresponse and is downregulated by p53 in colorectal cancer cell. Cancer Biol Ther. 2013;14(3):213–21.
102. Wang W, et al. Overexpression of high mobility group box 1 and 2 is associated with the progression and angiogenesis of human bladder carcinoma. Oncol Lett. 2013;5(3):884–8.
103. Boyer MJ, et al. Endothelial cell-derived extracellular vesicles alter vascular smooth muscle cell phenotype through high-mobility group box proteins. J Extracell Vesicles. 2020;9(1):1781427.
104. Sharma N, et al. Defining the Soluble and Extracellular Vesicle Protein Compartments of Plasma Using In-Depth Mass Spectrometry-Based Proteomics. J Proteome Res. 2024;23(9):4114–27.
105. Yu L, et al. Critical role of DEK and its regulation in tumorigenesis and metastasis of hepatocellular carcinoma. Oncotarget. 2016;7(18):26844–55.
106. Datta A, et al. Oncoprotein DEK as a tissue and urinary biomarker for bladder cancer. BMC Cancer. 2011;11:234.
107. Xu L, et al. Ribosomal protein L8 regulates the expression and splicing pattern of genes associated with cancer-related pathways. Turk J Biol. 2023;47(5):313–24.
108. Tripathi BK, et al. The pro-oncogenic noncanonical activity of a RAS•GTP:RanGAP1 complex facilitates nuclear protein export. Nat Cancer. 2024;5(12):1902–18.
109. Chavan S, et al. RanGTPase links nucleo-cytoplasmic transport to the recruitment of cargoes into small extracellular vesicles. Cell Mol Life Sci. 2022;79(7):392.
110. Zheng X, et al. Serine/arginine-rich splicing factors: the bridge linking alternative splicing and cancer. Int J Biol Sci. 2020;16(13):2442–53.
111. Zeng J, et al. CD46 splice variant enhances translation of specific mRNAs linked to an aggressive tumor cell phenotype in bladder cancer. Mol Ther Nucleic Acids. 2021;24:140–53.
112. Wu Q, et al. SRSF1-mediated alternative splicing regulates bladder cancer progression and cisplatin sensitivity through HIF1A/BNIP3/mitophagy axis. J Transl Med. 2025;23(1):571.
113. Chen TY, et al. Extracellular vesicles carry distinct proteo-transcriptomic signatures that are different from their cancer cell of origin. iScience. 2022;25(6):104414.
114. Lv L, et al. The DNA methylation-regulated miR-193a-3p dictates the multichemoresistance of bladder cancer via repression of SRSF2/PLAU/HIC2 expression. Cell Death Dis. 2014;5(9):e1402.
115. Samardzija P, et al. Defining the interactome of the pancreas-specific SPCA2 isoform (SPCA2C) identifies unique links to store-operated Ca(2+) entry. Febs J. 2025;(292):6644–69.
116. Li Y, et al. Urinary extracellular vesicle N-glycomics identifies diagnostic glycosignatures for bladder cancer. Nat Commun. 2025;16(1):2292.
117. Georgopoulos NT, et al. Immortalisation of normal human urothelial cells compromises differentiation capacity. Eur Urol. 2011;60(1):141–9.
118. Hoffmann MJ, et al. The New Immortalized Uroepithelial Cell Line HBLAK Contains Defined Genetic Aberrations Typical of Early Stage Urothelial Tumors. Bladder Cancer. 2016;2(4):449–63.
119. Mullenders J, et al. Mouse and human urothelial cancer organoids: A tool for bladder cancer research. Proc Natl Acad Sci U S A. 2019;116(10):4567–74.
120. Birhanu AG. Mass spectrometry-based proteomics as an emerging tool in clinical laboratories. Clin Proteom. 2023;20(1):32.
121. Boys EL, et al. Clinical applications of mass spectrometry-based proteomics in cancer: Where are we? Proteomics. 2023;23(7–8):e2200238.
122. Lynch KL. Accreditation and Quality Assurance for Clinical Liquid Chromatography-Mass Spectrometry Laboratories. Clin Lab Med. 2018;38(3):515–26.
123. Seger C, Salzmann L. After another decade: LC-MS/MS became routine in clinical diagnostics. Clin Biochem. 2020;82:2–11.
124. Arioz F, Tezcan S, Memboeuf A. The use of mass spectrometry in preclinical and clinical studies in oncology: a Mini Review. Analytical Letters. 2026;1–20.
125. Lu Y, et al. Recent progress in mass spectrometry-based liquid biopsy for cancer detection and analysis: A comprehensive review. TRAC Trends Anal Chem. 2025;190:118291.
126. Wenk D, et al. Recent developments in mass-spectrometry-based targeted proteomics of clinical cancer biomarkers. Clin Proteomics. 2024;21(1):6.
127. Dorayappan KDP, et al. A Microfluidic Chip Enables Isolation of Exosomes and Establishment of Their Protein Profiles and Associated Signaling Pathways in Ovarian Cancer. Cancer Res. 2019;79(13):3503–13.
128. Reátegui E, et al. Engineered nanointerfaces for microfluidic isolation and molecular profiling of tumor-specific extracellular vesicles. Nat Commun. 2018;9(1):175.
129. Sun N, et al. Purification of HCC-specific extracellular vesicles on nanosubstrates for early HCC detection by digital scoring. Nat Commun. 2020;11(1):4489.

Publisher's note

Springer Nature remains neutral with regard to jurisdictional claims in published maps and institutional affiliations.